Since January 2020 Elsevier has created a COVID-19 resource centre with free information in English and Mandarin on the novel coronavirus COVID-19. The COVID-19 resource centre is hosted on Elsevier Connect, the company's public news and information website.

Veterinary Microbiology 207 (2017) 248–258

Contents lists available at ScienceDirect

Veterinary Microbiology

journal homepage: www.elsevier.com/locate/vetmic

Genetic characteristics, pathogenicity, and immunogenicity associated with cell adaptation of a virulent genotype 2b porcine epidemic diarrhea virus

Sunhee Lee[a], Kyu-Yeol Son[b], Yun-Hee Noh[b], Seung-Chul Lee[b], Hwan-Won Choi[b], In-Joong Yoon[b], Changhee Lee[a,*]

[a] Animal Virology Laboratory, School of Life Sciences, BK21 Plus KNU Creative BioResearch Group, Kyungpook National University, Daegu 41566, Republic of Korea
[b] Choongang Vaccine Laboratory, Daejeon 34055, Republic of Korea

ARTICLE INFO

Keywords:
PEDV
Virulent genogroup G2b
Cell adaptation
Genome-wide sequencing
Deletions
ORF3
Pathogenicity
Attenuation

ABSTRACT

Porcine epidemic diarrhea virus (PEDV) has emerged or re-emerged worldwide, posing a significant financial threat to major pig-producing countries. In the present study, a virulent Korean pandemic PEDV strain, KNU-141112, was serially propagated in Vero cells for up to 100 passages. Through cell culture adaptation, we obtained four distinct deletion (DEL) mutants by plaque purification followed by nucleotide sequencing of the spike (S)/ORF3 gene-coding region, which were designated KNU-141112-S DEL2, −S DEL5, −S DEL2/ORF3, and −S DEL5/ORF3. Further whole genome sequencing identified 12 or 14 amino acid changes in the cell-adapted DEL strains. Animal inoculation studies revealed that the virulence of both S DEL2/ORF3 and S DEL5/ORF3 viruses with a large 46-nt deletion in the intergenic portion of S and ORF3 was remarkably diminished, indicating viral attenuation in the natural host. Furthermore, these cell-adapted strains elicited potent neutralizing antibody responses in immunized pigs. Taken together, our data indicate that the cell-attenuated S DEL2/ORF3 and S DEL5/ORF3 strains are promising candidates for the development of a safe and effective live PEDV vaccine.

1. Introduction

Porcine epidemic diarrhea (PED) is a deadly and highly contagious enteric pig disease that is characterized by acute watery diarrhea/vomiting, and dehydration, resulting in high mortality in newborn piglets (Lee, 2015; Saif et al., 2012). PED virus (PEDV), the etiological agent of PED, is a large, enveloped, single-stranded, positive-sense RNA virus that belongs to the genus *Alphacoronavirus* in the family *Coronaviridae* of the order *Nidovirales* (Pensaert and Debouck, 1978; Lee, 2015). The PEDV genome is approximately 28 kb in length with a 5′ cap and a 3′ polyadenylated tail, and is composed of a 5′-untranslated region (UTR), at least seven open reading frames (ORFs) designated ORF1a, ORF1b, and ORFs 2 through 6, and a 3′-UTR (Pensaert and Debouck, 1978; Kocherhans et al., 2001; Saif et al., 2012). The first two large ORFs, ORF1a and 1b, encode replicase polyproteins, pp la and pp 1ab, which undergo autoproteolysis by viral proteases to eventually produce 16 processing nonstructural proteins (nsp1–16). The remaining ORFs code for the four canonical structural spike (S), membrane (M), envelope (E), and nucleocapsid (N) proteins of coronaviruses and a single accessory gene, ORF3 (Lai et al., 2007; Lee, 2015). On the basis of phylogenetic analysis of the S gene, PEDV can be divided into two genotypes, designated genogroup 1 (G1; classical or recombinant and low-pathogenic) and genogroup 2 (G2; field epidemic or pandemic and high-pathogenic), which are genetically and antigenically distinct. Each genogroup is composed of two subgroups, 1a and 1b, and 2a and 2b, respectively (Lee, 2015; Lee et al., 2010; Lee and Lee, 2014; Oh et al., 2014).

Although PED outbreaks have been reported in Europe and Asia, the veterinary health impact and related economic losses have been most devastating in Asian swine-producing nations in the past two decades. Despite its notorious reputation in Asia, PED was not well-recognized worldwide until the disease hit the United States (US) in 2013. Since its emergence in the US, PEDV has spread quickly throughout most of the states and to adjacent countries, sustaining a tremendous threat in the North American pork business (Mole, 2013; Stevenson et al., 2013; Vlasova et al., 2014). Subsequently, large, severe PED outbreaks recurred almost simultaneously in South Korea, Japan, and Taiwan, and US prototype-like G2b PEDV strains were found to be accountable for these recent epizootics (Lee and Lee, 2014; Lin et al., 2014; Suzuki et al., 2015). Furthermore, recombinant G1b or pandemic G2b PEDVs re-emerged throughout western and central Europe (Boniotti et al., 2016; Dastjerdi et al., 2015; Grasland et al., 2015; Hanke et al., 2015;

* Corresponding author at: School of Life Sciences, College of Natural Sciences, Kyungpook National University, Daegu 41566, Republic of Korea.
E-mail address: changhee@knu.ac.kr (C. Lee).

http://dx.doi.org/10.1016/j.vetmic.2017.06.019
Received 30 March 2017; Received in revised form 27 June 2017; Accepted 27 June 2017

Mesquita et al., 2015; Steinrigl et al., 2015; Theuns et al., 2015). Therefore, PED has become a globally emerging and re-emerging viral swine disease that causes enormous financial damage throughout the world and is considered one of the most economically important diseases in countries with intensive swine industries.

A PED epizootic in South Korea was first reported in 1992 (Kweon et al., 1993). Since that time, PED has remained rampant, devastating the domestic hog industry. More recently, the 2013–2014 PED epidemic swept through mainland South Korea, followed by Jeju Island, and killed hundreds of thousands of piglets in domestic herds (Lee et al., 2014a; Lee and Lee, 2014). Currently, a limited number of PEDV vaccines, either modified live or inactivated/killed, are commercially available in South Korea. These vaccines contain a single G1a classical strain (Korean SM98-1 or DR-13 strains, or Japanese 83P-5) and, in many cases, are not fully protective against genetically divergent field strains. The incomplete efficacies of current PEDV vaccines might be ascribed to antigenic or genetic differences between the major S glycoprotein of the vaccine and field epidemic strains (Kim et al., 2015; Lee, 2015; Lee et al., 2010, 2014a; Lee and Lee, 2014; Oh et al., 2014). Considering these issues, there is a strong demand for a new vaccine to be developed against G2b epizootic or related strains prevalent in the field. In general, attenuation of the virulence of a wild-type virus can be achieved by sequential passage in non-host cell lines. The attenuated virus can be explored to prepare a modified live virus (MLV) vaccine. Indeed, current live PEDV vaccines were created by continuous passages of classical G1a strains in African green monkey kidney-derived Vero cells (Kweon et al., 1999; Sato et al., 2011; Song et al., 2007). In the present study, a highly virulent Korean G2b strain KOR/KNU-141112/2014 was serially propagated in Vero cells for up to 100 passages for attenuation so that it could be further used for the development of an MLV vaccine.

2. Materials and methods

2.1. Cells, virus, and antibody

Vero cells (ATCC CCL-81) were cultured in alpha minimum essential medium (α-MEM; Invitrogen, Carlsbad, CA) with 5% fetal bovine serum (FBS; Invitrogen) and antibiotic-antimycotic solutions (100×; Invitrogen) and maintained at 37 °C in a humidified 5% CO_2 incubator. Virulent Korean PEDV strain KOR/KNU-141112/2014 was isolated and propagated in Vero cells as described previously (Lee et al., 2015). A viral stock was prepared from the 5th passage in cell culture (KNU-141112-P5) and used as the parental virus in this study (GenBank accession no. KR873434). PEDV N protein-specific monoclonal antibody (MAb) was obtained from ChoogAng Vaccine Laboratory (CAVAC; Daejeon, South Korea).

2.2. Serial passage of the virus

PEDV strain KNU-141112-P5 was plaque purified twice in Vero cells, and the purified virus was continuously passaged on Vero cells as described previously with some modifications (Lee et al., 2015). Confluent Vero cells grown in 100-mm diameter tissue culture dishes were washed with PBS and inoculated with 1 ml of 10-fold diluted PEDV KNU-141112 with trypsin (USB, Cleveland, OH). After incubation at 37 °C for 1 h, 7 ml of virus growth medium [α-MEM supplemented with antibiotic-antimycotic solutions, 0.3% tryptose phosphate broth (TPB; Sigma, St. Louis, MO), 0.02% yeast extract (Difco, Detroit, MI), 10 mM HEPES (Invitrogen), and 5 μg/ml of trypsin] was added. The inoculated cells were maintained at 37 °C under 5% CO_2 and monitored daily for cytopathic effect (CPE). When ~70% of cells showed CPE, the inoculated cells were subjected to three rounds of freezing and thawing. The culture supernatants were then centrifuged for 10 min at 400 × *g* (Hanil Centrifuge FLETA5, Incheon, South Korea) and filtered through a 0.45-μm pore-size filter (Millipore, Billerica, MA). The clarified supernatants were aliquoted and stored at −80 °C as the viral stock for the next passage. In the same manner, 100 subsequent passages were performed in Vero cells. Beginning at the 70th passage in cell culture, the virus was plaque cloned every 10 passages. Single plaques were chosen and subjected to nucleotide (nt) sequencing to identify mutations in the S gene, and the selected viruses were further passaged.

2.3. Immunofluorescence assay (IFA)

Vero cells grown on microscope coverslips placed in 6-well tissue culture plates were infected with PEDV at a multiplicity of infection (MOI) of 0.1. The virus-infected cells were subsequently cultured until 24 hpi, fixed with 4% paraformaldehyde for 10 min at room temperature (RT) and permeabilized with 0.2% Triton X-100 in PBS at RT for 10 min. The cells were blocked with 1% bovine serum albumin (BSA) in PBS for 30 min at RT and then incubated with N-specific MAb for 2 h. After being washed five times in PBS, the cells were incubated for 1 h at RT with a goat anti-mouse secondary antibody conjugated to Alexa Fluor 488 (Invitrogen), followed by counterstaining with 4′,6-diamidino-2-phenylindole (DAPI; Sigma). The coverslips were mounted on glass microscope slides in mounting buffer, and cell staining was visualized using a fluorescence Leica DM IL LED microscope (Leica, Wetzlar, Germany).

2.4. Virus titration

Vero cells were infected with each KNU-141112 virus stock in the presence of trypsin as described above. The culture supernatants were collected at 24 or 48 h postinfection (hpi), when 70% CPE commonly developed. For the growth kinetics experiments, supernatants were harvested from cells infected with each virus strain at various time points (6, 12, 24, 36, and 48 hpi) and stored at −80 °C. Virus titers were measured in duplicate by plaque assay using Vero cells and defined as plaque-forming units (PFU) per ml. In brief, Vero cells grown in 6-well plates were inoculated with 200 μl/well of 10-fold serially diluted virus suspensions containing trypsin and adsorbed for 1 h at 37 °C. The inoculated cells were overlaid with 2 ml of premixed virus growth medium and 1.5% Bacto Agar (Difco) and incubated for 2 days at 37 °C. Plaque morphologies were assessed by staining with 1% crystal violet in ethanol at 48 hpi.

2.5. Nucleotide sequence analysis

The full-length genomic sequences of cell adapted KNU-141112 DEL strains were determined by next-generation sequencing (NGS) technology. Total RNA was extracted from each virus stock serially passaged in Vero cells using a RNeasy Mini Kit (Qiagen, Hilden, Germany) according to the manufacturer's instructions and was used as a template to amplify cDNA fragments as described elsewhere (Lee and Lee, 2014; Lee et al., 2014b, 2015). Ten overlapping cDNA fragments encompassing the entire genome of each virus strain were generated, pooled in equimolar amounts, and subjected to NGS using the Ion Torrent Personal Genome Machine (PGM) Sequencer System (Life Technologies, Carlsbad, CA) and a 316 v2 sequencing chip (Life Technologies) as described previously (Lee and Lee, 2014; Rothberg et al., 2011). The single-nucleotide variants (SNVs) were analyzed using CLC Genomic Workbench version 7.0 (CLC Bio, Cambridge, MA), and the individual NGS reads were assembled using the complete genome of PEDV strain KNU-141112-P5 (GenBank accession no. KR873434) as a reference. The 5′ and 3′ ends of the genomes of cell-adapted KNU-141112 strains were determined by rapid amplification of cDNA ends (RACE) as described previously (Lee and Lee, 2013). The full-length genomic nt sequences of high passage KNU-141112 DEL derivatives (KNU-141112-S DEL2, –S DEL2/ORF3, –S DEL5, and –S DEL5/ORF3) were deposited in the GenBank database under accession numbers KY825240 to KY825243, respectively. In addition, the unique nt deletions identified in S and/or

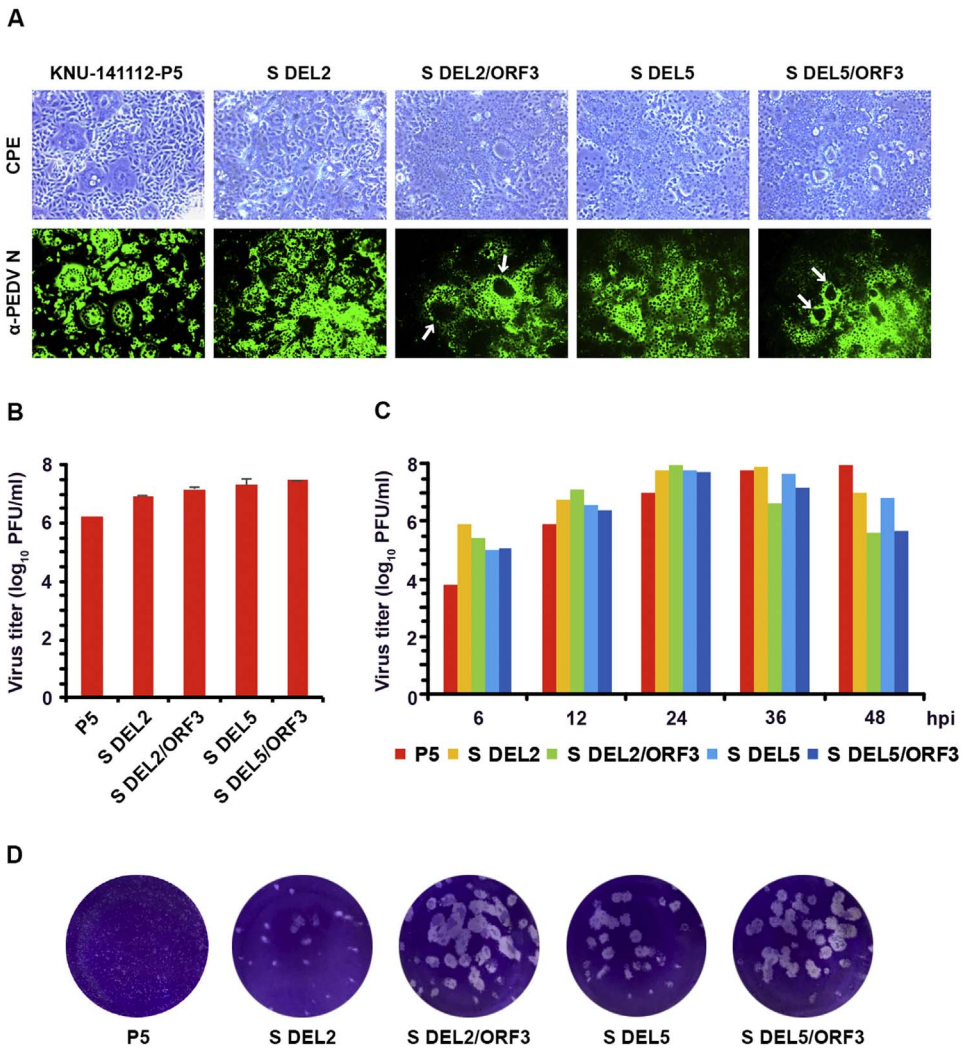

Fig. 1. Cytopathology and growth properties of virulent PEDV isolate KNU-141112 and cell-adapted DEL strains in infected Vero cells. (A) CPE formation in Vero cells infected with KNU-141112-P5 and cell-adapted DEL viruses. PEDV-specific CPE was observed daily, and cells were photographed at 24 hpi using an inverted microscope at a magnification of 200× (upper panels). For immunostaining, infected cells were fixed at 24 hpi and incubated with MAb against the N protein, followed by incubation with Alexa green-conjugated goat anti-mouse secondary antibody. The cells were then examined under a fluorescence microscope at 200× magnification (lower panels). Arrows indicate distinct vacuolations in Vero cells infected with strain S DEL2/ORF3 or S DEL5/ORF3. (B) Virus titers of the parental KNU-141112-P5 and cell-adapted DEL strains. At 24 or 48 hpi, the virus supernatants were collected and virus titers were determined by plaque assay. (C) One-step growth kinetics for KNU-141112 strains. At the indicated time points post-infection, culture supernatants were harvested, and virus titers were determined by plaque assay. Results are expressed as the mean values from duplicating testing in two independent experiments and error bars represent standard deviations. (D) Viral plaque morphology of the parental and cell-adapted viruses. Monolayers of Vero cells grown in 6-well plates were infected with each virus. The cells were overlaid with 0.75% agarose and incubated for 2 additional days. Plaques were stained with 1% crystal violet at 48 hpi and photographed.

ORF3 were verified using the traditional Sanger method. Two or three overlapping cDNA fragments spanning the entire S gene and ORF3 regions of each strain were RT-PCR amplified as described previously (Lee et al., 2010). The individual cDNA amplicons were gel purified, cloned into a pGEM-T Easy Vector System (Promega, Madison, WI), and sequenced in both directions using two commercial vector-specific T7 and SP6 primers and viral gene-specific primers.

2.6. Phylogenetic analysis

The sequences of 36 fully sequenced S genes and 30 complete genomes of PEDV isolates were independently used in sequence alignments and phylogenetic analyses. The multiple-sequencing alignments were generated in the ClustalX 2.0 (Thompson et al., 1997) and the percentages of nt sequence divergences were further assessed using the same software. Phylogenetic trees were constructed from the aligned nt or amino acid (aa) sequences using the neighbor-joining method and subsequently subjected to a bootstrap analysis with 1000 replicates to determine the percentage reliability at each internal node of the trees (Saitou and Nei, 1987). All tree figures were produced using Mega 4.0 software (Tamura et al., 2007).

2.7. Pig infection experiments

The *in vivo* swine studies described here were performed at the Choongang Vaccine Laboratory Animal Facility under the guidelines established by its Institutional Animal Care and Use Committee. A total of 14 suckling piglets of 3 days of age were obtained from commercial crossbred sows (Great Yorkshire × Dutch Landrace) at a conventional breeding farm with a good health record and either vaccination against PEDV or no known prior PED outbreak. All animals were confirmed negative for PEDV, transmissible gastroenteritis virus (TGEV), porcine deltacoronavirus, and porcine rotaviruses by virus-specific RT-PCRs of rectal swabs and determined to be free of antibodies to PEDV, as well as to TGEV and porcine reproductive and respiratory syndrome virus. Pigs were randomly assigned to four experimental groups: the parental KNU-141112-P5-inoculated (n = 3), KNU-141112-S DEL2/ORF3-inoculated (n = 4), KNU-141112-S DEL5/ORF3-inoculated (n = 4), and sham-inoculated control (n = 3) groups. Animals were fed commercial milk replacer frequently (3 to 4 times daily) and had *ad libitum* access to water for the duration of the study (8 days). Following a 2-day acclimation period, piglets (5 days old) in the virus-inoculated groups received a 1 ml dose of $10^{5.0}$ $TCID_{50}$/ml (equivalent to 100 median lethal doses LD_{50} of KNU-141112) of one of the viruses orally (Baek et al., 2016; Lee et al., 2015). The sham-inoculated pigs were administered cell culture media as a placebo. Animals were monitored daily for clinical signs of vomiting, diarrhea, and mortality throughout the experiment. Stool samples from pigs in all groups were collected prior to inoculation and daily with 16-inch cotton-tipped swabs and subjected to RT-PCR using an *i*-TGE/PED Detection Kit (iNtRON Biotechnology, Seongnam, South Korea) and real-time RT-PCR to detect the presence of PEDV shedding. A clinical significance score (CSS) was determined with the following scoring criteria based on visual examination for 7 days post-inoculation (DPI) used to measure diarrheal severity: 0, normal

Table 1
Summary of amino acid mutations among the parental KNU-141112-P5 and the DEL derivative viruses during *in vitro* serial passages.

ORFs	Encoding protein	aa (aa length)	P5 position[a]	S DEL2	S DEL2/ ORF3	S DEL5	S DEL5/ ORF3
ORF1a	nsp2 (774)	192	T	T	T	I	T
	nsp3 (1,621)	1564	S	F	F	F	F
		2178	I	L	L	I	I
		2182	C	F	F	C	C
	nsp5 (302)	3186	T	I	I	I	I
ORF1b	nsp12 (927)	142	K	N	K	K	K
	nsp13 (597	1025	T	I	T	I	I
		1165	A	A	A	S	S
ORF2	S (1,386)	272	K	T	T	T	T
		381	N	N	K	N	N
		383	T	N	T	N	N
		516	T	T	I	T	T
		888	G	R	R	R	R
		1287	E	Q	Q	Q	Q
		1380	F	F	H	F	H
		1381	E	E	D	E	D
ORF3	ORF3 (224)	26	D	Y	–[b]	Y	–
		135	K	K	S	K	K
		166	N	S	–	S	S
ORF4	E (76)	70	P	S	S	S	S
Total no. of nt/aa changes				22/14	28/14	19/12	19/12

[a] Amino acid position numbering is based on the sequence of KNU-141112-P5 strain.
[b] This is the deleted region in ORF3.

and no diarrhea (mean cycle threshold [Ct] values of > 45); 1, mild and fluidic feces; 2, moderate watery diarrhea; 3, severe watery and projectile diarrhea (mean Ct values of < 20); 4, death. Piglets were necropsied upon death after challenge throughout the study, whereas all surviving pigs from the challenge and control groups were euthanized at 7 days post-challenge for post-mortem examinations.

To assess immunogenicity, a total of 11 3-week-old pigs were obtained and tested to confirm that they were not infected with PEDV-related viruses as described above. Pigs were randomly allocated into the parental KNU-141112-P5-inoculated (n = 3), KNU-141112-S DEL2/ORF3-inoculated (n = 3), KNU-141112-S DEL5/ORF3-inoculated (n = 3), and sham-inoculated control (n = 2) groups. After 2 days of acclimation, 9 pigs (24 days old) were immunized orally with 1 ml of one of the viruses and boosted once with the same virus after a 2-week interval. Two pigs were sham inoculated and boosted with cell culture media. Pre-immune sera were collected before the first immunization, and antisera were collected at 2 weeks after the final boost. Serum samples were tested for PEDV antibody using a virus neutralization assay.

2.8. Quantitative real-time RT-PCR

Viral RNA was extracted from fecal samples prepared as described above using an *i*-TGE/PED Detection Kit according to the manufacturer's protocol. Quantitative real-time RT-PCR was performed using a One Step SYBR PrimeScript RT-PCR Kit (TaKaRa, Otsu, Japan) and primers (forward primer 5′-ACGTCCCTTTACTTTCAATTCACA-3′, reverse primer 5′-TATACTTGGTACACACATCCAGAGTCA-3′) and a probe (5′-FAM-TGAGTTGATTACTGGCACGCCTAAACCAC-BHQ1-3′) described elsewhere (Kim et al., 2007; Sagong and Lee, 2011). The reaction was performed using a Thermal Cycler Dice Real Time System (TaKaRa) according to the manufacturer's protocol under the following conditions: 1 cycle of 45 °C for 30 min, 1 cycle of 95 °C for 10 min, and 40 cycles of 95 °C for 15 s and 60 °C for 1 min. The results were analyzed using the system software as described previously (Sagong and Lee, 2011). A PEDV isolate with a known infectivity titer was 10-fold serially diluted to generate a standard curve in each PCR plate. The virus concentrations ($TCID_{50}$/ml) in samples were calculated based on the standard curve. The mean Ct values were calculated based on PCR positive samples, and the mean virus titers were calculated based on all pigs within the group.

2.9. Histopathology and immunohistochemistry of the small intestines

At necropsy, small intestinal tissue specimens (< 3 mm thick) collected from each piglet were fixed with 10% formalin for 24 h at RT and embedded in paraffin according to standard laboratory procedures. The formalin-fixed paraffin-embedded tissues were cut in 5–8-μm thick sections on a microtome (Leica), floated in a 40 °C water bath containing distilled water, and transferred to glass slides. The tissues were then deparaffinized in xylene for 5 min and washed in decreasing concentrations of ethanol (100%, 95%, 90%, 80%, and 70%) for 3 min each. The deparaffinized intestinal tissue sections were stained with hematoxylin and eosin (Sigma) for histopathology or subjected to immunohistochemistry (IHC) using PEDV N-specific MAb as described previously (Lee et al., 2015). Briefly, the paraffin-embedded tissue sections were deparaffinized, treated with 0.01 M citrate buffer (pH 6.0) in a microwave oven for 5 min, chilled at RT for 20 min, and then incubated with 0.3% hydrogen peroxide in distilled water for 20 min to block endogenous peroxidase. The sections were washed three times in PBS, blocked with normal horse serum (VECTASTAIN ABC Kit; Vector Laboratories, Burlingame, CA), and incubated for 1 h at RT with N-specific MAb. After rinsing in PBS, the samples were reacted for 45 min at RT with a horse anti-mouse secondary antibody (VECTASTAIN ABC Kit), incubated with avidin-biotin peroxidase complex for 45 min (VECTASTAIN ABC Kit), and developed using the DAB Substrate Kit (Vector Laboratories) according to the manufacturer's instructions. The slides were then counterstained with hematoxylin, dehydrated, cleared with xylene, and mounted on microscope glass slides in mounting buffer, and tissue staining was visualized using a microscope.

2.10. Serum neutralization

The presence of PEDV-specific neutralizing antibodies in serum samples collected from pigs in all groups was determined using a serum neutralization (SN) test in 96-well microtiter plates using PEDV isolate KNU-141112 as previously described (Oh et al., 2014) with minor modifications. Briefly, Vero cells were grown at 2×10^4/well in 96-well tissue culture plates for 1 day. The KNU-141112-P5 virus stock was diluted in serum-free α-MEM to make 200 $TCID_{50}$ in a 50-μl volume. The diluted virus was then mixed with 50 μl of 2-fold serial dilutions of each inactivated serum sample in 96-well plates and incubated at 37 °C for 1 h. The mixture was inoculated into Vero cells and incubated at 37 °C for 1 h. After removing the mixture, the cells were thoroughly rinsed five times with PBS and maintained in virus growth medium at 37 °C in a 5% CO_2 incubator for 2 days. The neutralization titer was calculated as the reciprocal of the highest dilution of serum that inhibited virus-specific CPE in duplicate wells.

2.11. Statistical analysis

A student's t test was used for all statistical analyses, and P-values of less than 0.05 were considered statistically significant.

3. Results

3.1. Phenotypic characteristics of cell-adapted DEL strains were altered in vitro

Previously, we isolated the virulent G2b strain KOR/KNU-141112/2014 liable for the recent immense PEDV epidemics in South Korea (Lee et al., 2015). In the current study, we initially conducted *in vitro* serial propagation and plaque cloning at selected passages. For plaque purification of high-passage derivatives of KNU-141112, single plaques of KNU-141112-P80 and –P90 (80th and 90th passage of KNU-141112, respectively) were picked, and the nt sequences of the full-length S genes were individually determined. Preliminary nt sequencing initially identified four different patterns of deletions (DEL): a 6-nt (two amino acids) DEL in the N-terminus of S1 (S DEL2), 15-nt (five amino acids) DEL in the N-terminus of S1 (S DEL2), S DEL2 plus a large 46-nt deletion of the intergenic junction between the C-terminus of S and N-terminus of ORF3 (S DEL2/ORF3), and S DEL5 plus the identical deletion (S DEL5/ORF3). The plaque-cloned viruses with the individual DEL patterns were further propagated up to 100 passages to produce virus stocks that were designated KNU-141112-S DEL2, KNU-141112-S DEL5, KNU-141112-S DEL2/ORF3, and KNU-141112-S DEL5/ORF3.

Like the parental virus, all cell-adapted DEL strains were capable of producing PEDV archetypal CPE, such as cell fusion, multi-nucleated cell formation (syncytium or polykaryon), and detachment, in infected Vero cells. CPE onset occurred at 12 hpi, and prominent CPE was observed within 24 hpi for the parental and cell-adapted viruses. Virus propagation was confirmed by detecting PEDV antigens by IFA using a PEDV N-specific MAb. The distinct staining was distributed throughout the cytoplasm in typical syncytial cells (Fig. 1A). Attractively, the DEL strains caused noticeable CPE and IFA staining showing vacuolation and syncytia in giant multi-nucleated cells that were bigger and more predominant in cells infected with KNU-141112-S DEL2/ORF3 and KNU-141112-S DEL5/ORF3 (Fig. 1A, arrows).

To investigate the *in vitro* phenotypic traits of serially passaged DEL strains, the amounts of infectious virus were assessed by virus titration. The infectious titer of the parental KNU-141112-P5 was determined to be $10^{6.20}$ PFU/ml, whereas the cell-adapted virus titers ranged from $10^{6.92}$ to $10^{7.47}$ PFU/ml (Fig. 1B). One-step growth curves revealed that growth of the parental virus increased gradually and reached a peak titer at 48 hpi (Fig. 1C). In contrast, growth kinetics of the cell-passaged DEL strains were faster and titers were higher until 24 or 36 hpi, relative to the parental strain. Furthermore, all DEL strains attained their highest titers at 24 hpi, and titers decreased thereafter. We next investigated the plaque morphologies of the KNU-141112 strains. As shown in Fig. 1D, viral plaques from the cell-adapted DEL strains were enlarged in compared to those of the parental virus, and among them, the KNU-141112-S DEL2/ORF3 and KNU-141112-S DEL5/ORF3 viruses produced the largest plaques. These results indicated that each DEL signature that arose during cell adaptation was independently

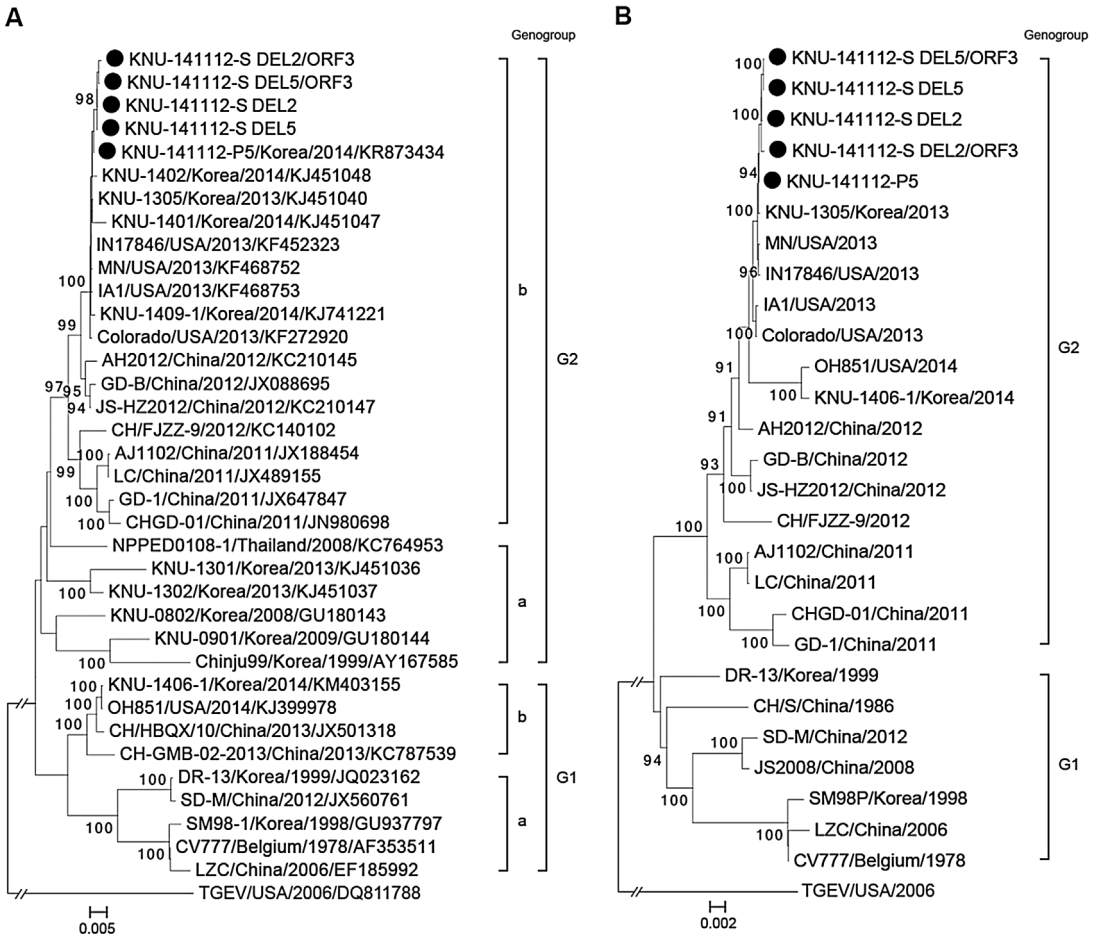

Fig. 2. Phylogenetic analyses of the nucleotide sequences of the spike genes (A) and full-length genomes (B) of PEDV strains. A region of the spike protein and the complete genome sequence of TGEV were included as outgroup in each tree. Multiple-sequence alignments were performed in ClustalX, and the phylogenetic tree was constructed from the aligned nucleotide sequences using the neighbor-joining method. Numbers at each branch represent bootstrap values greater than 50% based on 1000 replicates. Names of the strains, countries and years of isolation, GenBank accession numbers, and genogroups and subgroups proposed in this study are shown. The parental KNU-141112-P5 and cell-adapted DEL strains identified in this study are indicated by solid circles. Scale bars indicate nucleotide substitutions per site.

associated with increased viral fitness.

3.2. Whole genome sequencing showed mutations and unique deletions in highly cell-adapted DEL viruses

To investigate the genomic changes that may have accounted for the viral fitness gains during *in vitro* serial passage in Vero cells, the full-length nt sequences of the cell culture-passaged DEL strains were determined. Except for their own DEL pattern in the S gene and/or ORF3 of individual strains, no additional insertions and deletions were found throughout the genomes after cell culture passage. The 5′-UTRs of all DEL strains remained unchanged, whereas the 3′-UTR was completely conserved only in S DEL2. The remaining strains had a G to T substitution at a position 6 in the 3′ UTR (S DEL5 and S DEL5/ORF3) or A to T and G to A substitutions at positions 135 and 193 in the 3′ UTR (S DEL2/ORF3), respectively. The 100th-passage S DEL2 and S DEL2/ORF3 strains contained 14 aa changes that were distributed randomly throughout the genome, whereas the S DEL5 and S DEL5/ORF3 virus equally had 12 aa variations (Table 1). Overall, 28.6% to 42.9% (4–6 aa changes) of 12 or 14 non-silent mutations emerged in nsps, whereas 57.1% to 71.4% (7–10 aa changes) occurred in structural S and E and accessory ORF3 proteins. No mutations arose in the M and N protein-coding regions. Details in aa mutations among the parental KNU-141112-P5 and cell-adapted DEL strains are summarized in Table 1. Further phylogenetic analyses based on the entire genome and full-length S indicated that all cell-adapted DEL strains still belonged to subgroup G2b along with the parental virus and global epizootic strains (Fig. 2)

The most outstanding feature of the genetic alterations resulting from the serial passage of KNU-141112 in Vero cells was the emergence of extraordinarily small and/or large deletions in the high-passage (at least 70) viruses. The first DEL pattern was short 6-nt or 15-nt deletions in the S gene, resulting in 2-aa (S N-DEL2) or its extended 5-aa (S N-DEL5) deletions at positions 56–57 and 56–60, respectively at the N-terminus of S (Fig. 3A). The second DEL was a combination pattern by a large 46-nt deletion in the intergenic portion of S and ORF3 (nt positions 24,771–24,8l6), leading to a malfunction in the authentic termination and initiation of S and ORF3, respectively. As a result, an alternative TGA termination codon in S occurred at the 7th position downstream from the last T, just before the beginning of the deletion, creating a truncated S product with a 5-aa shorter cytoplasmic domain (S C-DEL5) with 2 aa mutations (F1380H and E1381D) at the last two positions of the S gene product compared to the parental virus (Fig. 3B). In addition, because the first start codon of ORF3 was interrupted, one of the two potential events could be anticipated: the disruption of ORF3 expression or the exploration of an alternative start codon for ORF3 expression. The former would result in no production of the corresponding protein, whereas the latter would instinctively promote the use of a second ATG initiator located 188 nt downstream from the deleted region, leading to the generation of an N-terminal-truncated ORF3 product with the 70-aa deletion (ORF3 N-DEL70) (Fig. 3C). The third type of DEL pattern was an uncommon DEL resulting from the substitution of GCT to TGA terminator sequence at positions 409–411 in ORF3 (25,202–25,204 at the genome level). These changes caused premature termination 264 nt upstream from the expected stop site, indirectly removing 88 aa residues in the C-terminus of ORF3 (ORF3C-

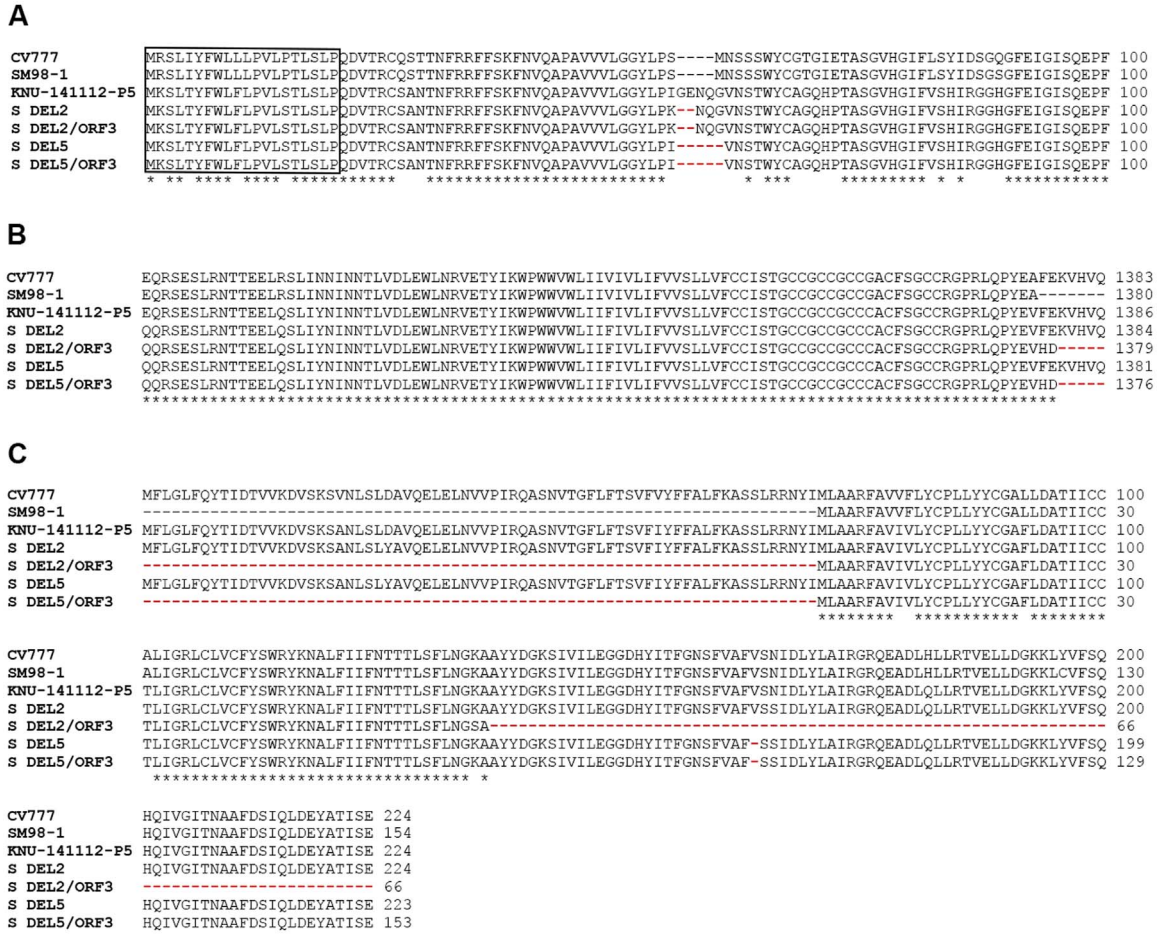

Fig. 3. Amino acid sequence alignments of the N-terminal (A) and C-terminal (B) regions of the S glycoprotein gene and the entire ORF3 protein (C) in PEDV G1a reference, parental KNU-141112-P5, and cell-adapted DEL strains. A solid box represents the putative signal peptide sequence. The dashes (−) indicate deleted sequences.

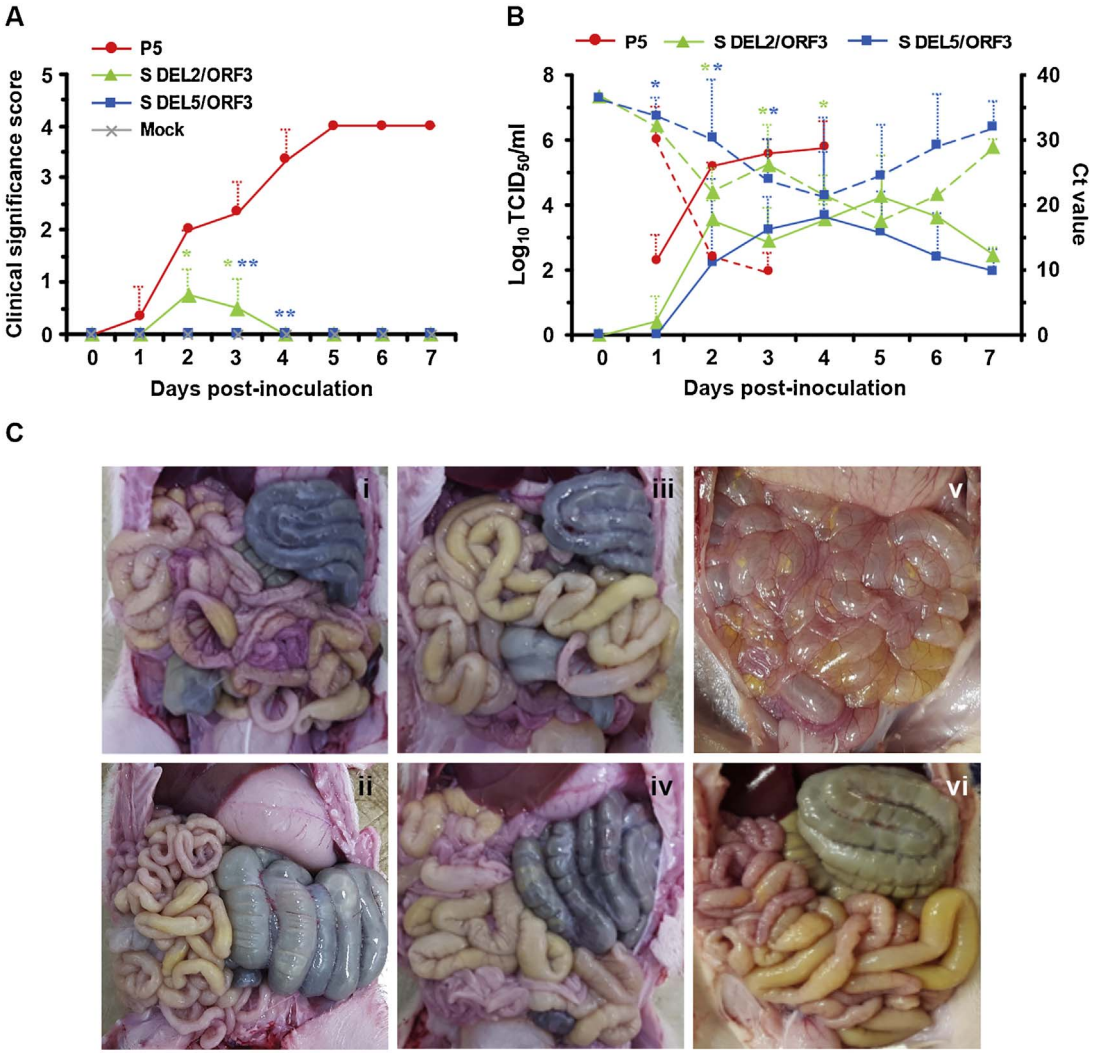

Fig. 4. Clinical significance scores, virus shedding, and macroscopic small intestine lesions in piglets from four groups. (A) Clinical significance scores were measured as described in the Materials and Methods section. (B) PEDV titers in rectal swap samples at each time point were determined by a quantitative real-time RT-PCR. The Ct values presented in the figure are mean Ct values from PCR-positive pigs (broken lines). The virus titers (log_{10} $TCID_{50}$/ml) are the mean virus titers from all pigs (solid lines). Error bars represent standard deviations. *P* values were calculated by comparing the parental virus- and cell-adapted DEL virus-inoculated groups using Student's *t* test. *, $P = 0.001$ to 0.05; **, $P < 0.001$. (C) Small intestines from representative pigs inoculated with S DEL2/ORF3 (panels i and ii), S DEL5/ORF3 (panels iii and iv), and KNU-141112-P5 (panel v), and a negative control animal (panel vi) were examined for gross lesions. Note that only piglets inoculated with the parental virus typical thin and transparent intestinal walls (panel v).

DEL88) (Fig. 3C). The DEL fourth signature was a minor 3-nt TCG deletion covering the codons for 2 residues, phenylalanine and valine, at positions 163 and 164 in the C-terminal portion of ORF3. The first two nt are located at the last two underlined positions of the TTC triplet for phenylalanine, whereas the last nt is placed at the first underlined position of the GTT codon for valine. Although this mutation led to a reading frame shift, the remaining first T and last TT of the triplets for phenylalanine and valine, respectively, created a new TTT triplet for phenylalanine, resulting in the single loss of the next valine residue at position 164 of ORF3, followed by recovery of the altered frame shift (ORF3 C-DEL1) with no further mutations (Fig. 2C). Finally, our whole genome sequencing data fully confirmed the DEL pattern of each cell-adapted strain: KNU-141112-S DEL2 (single S N-DEL2), KNU-141112-S DEL5 (S N-DEL5 and ORF3 C-DEL1), KNU-141112-S DEL2/ORF3 (S N-DEL2, a combination of S C-DEL5/ORF3 N-DEL70, and ORF3 C-DEL88), and KNU-141112-S DEL5/ORF3 (S N-DEL5, a combination of S C-DEL5/ORF3 N-DEL70, and ORF3 C-DEL1). On the basis of their own DEL pattern(s), therefore, the cell-adapted DEL strains were each predicted to encode S and ORF3 proteins with various lengths that were shorter than those of the parental strain (S, 1386 aa; ORF3, 224 aa): KNU-141112-S DEL2 (S, 1384 aa; ORF3, 224 aa), KNU-141112-S DEL5 (S, 1381 aa; ORF3, 223 aa), KNU-141112-S DEL2/ORF3 (S, 1379 aa; ORF3, 66 aa), and KNU-141112-S DEL5/ORF3 (S, 1376 aa; ORF3, 153 aa).

3.3. Highly cell-adapted DEL viruses were attenuated and immunogenic in vivo

Since high-passage derivatives of PEDV experimentally exhibit reduced pathogenicity in pigs, and a large deletion in the ORF3 region is present in attenuated or live vaccine strains (Park et al., 2008; Wang et al., 2012), the second and third DEL patterns (ORF3 N-DEL70 and ORF3 C-DEL88) identified in the present study are most likely associated with the virulence of KNU-141112. Thus, cell-adapted KNU-141112-S DEL2/ORF3 and KNU-141112-S DEL5/ORF3 strains were chosen for subsequent animal studies to assess the *in vivo* phenotypic changes associated with serial *in vitro* passage, a common tool for virus attenuation, of the virulent KNU-141112 strain. The pathogenicity of the parental KNU-141112-P5 and its cell-passaged derivatives, KNU-141112-S DEL2/ORF3 and KNU-141112-S DEL2/ORF3, was characterized in pigs. Fourteen piglets divided into four groups of three or four animals each were challenged orally with parental KNU-141112-

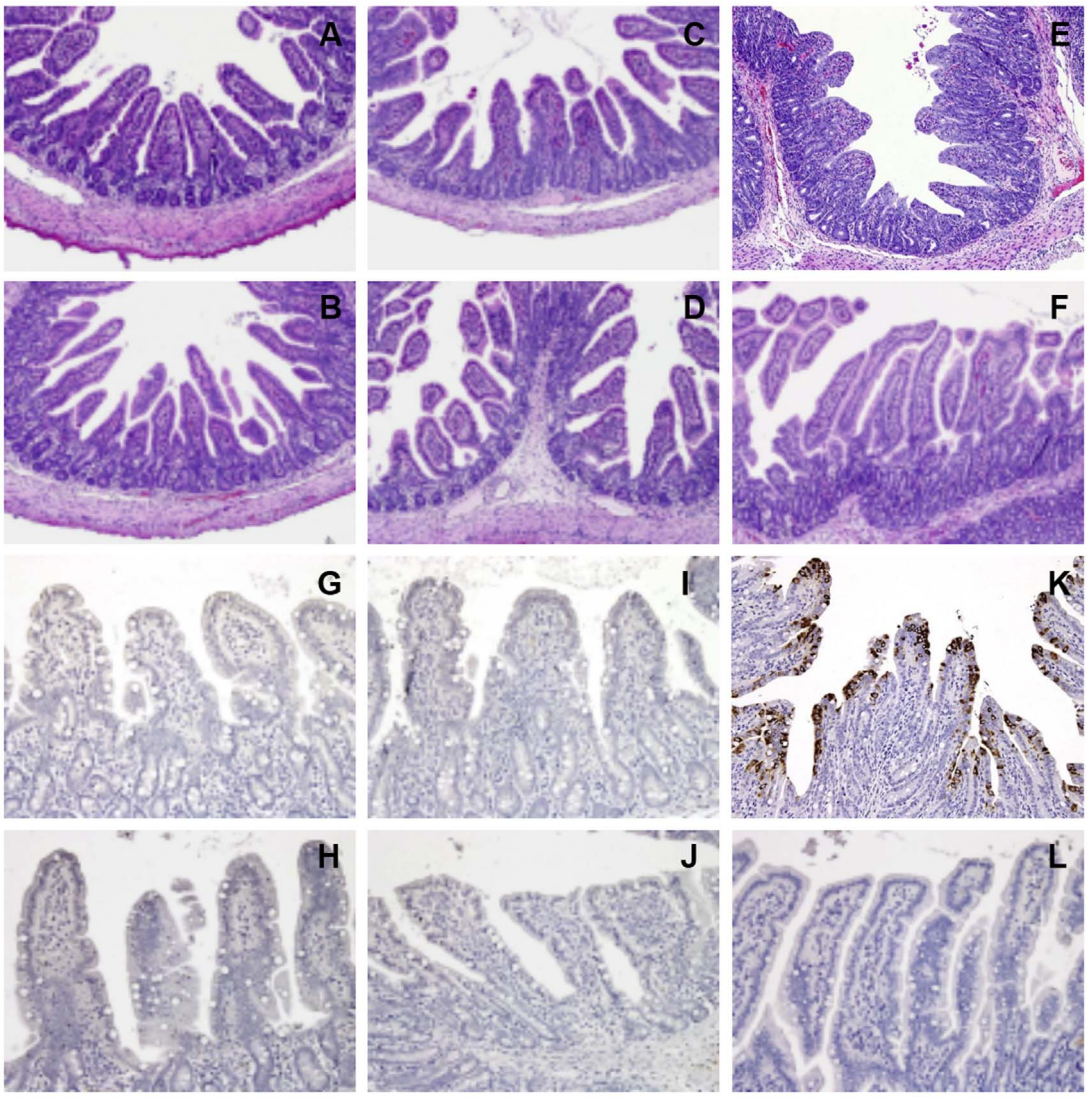

Fig. 5. Histopathology of the intestines of piglets inoculated with the parental and cell-adapted DEL strains. (A–F) Hematoxylin and eosin-stained tissue sections of the jejunums from virus-inoculated and negative-control pigs (100× magnification). Jejunums from piglets infected with the virulent KNU-141112-P5 strain showed acute diffuse, severe atrophic enteritis with vacuolation of superficial epithelial cells (panel E). The normal villous epithelium of the jejunums was recorded in pigs inoculated with KNU-141112-S DEL2/ORF3 (panels A and B) and –S DEL5/ORF3 (panels C and D), and a mock-inoculated piglet (panel F). (G–L) Detection of PEDV antigen by IHC analysis of jejunum tissue sections from virus-inoculated and negative-control pigs (200× magnification). PEDV antigen signals appear brown and were detected in epithelial cells in the jejunums of all PEDV KNU-141112-P5-inoculated piglets (panel K). No PEDV antigen was detected in the jejunums of piglets inoculated with KNU-141112-S DEL2/ORF3 (panels G and H) or –S DEL5/ORF3 (panels I and J), or a mock-inoculated piglet (panel L).

P5 (group 1), KNU-141112-S DEL2/ORF3 (group 2), or KNU-141112-S DEL5/ORF3 (group 3), and the remaining three piglets in a control group were inoculated with cell culture medium. Clinical signs were recorded daily, and fecal swabs were collected prior to and after challenge for the duration of the study. During the acclimation period, all piglets were active, showed no clinical symptoms, had normal fecal consistency, and no PEDV genetic material was detected by PEDV-specific RT-PCR in fecal samples from any piglet. Following challenge, none of the negative-control piglets developed clinical signs typical of PEDV throughout the pathogenicity study. In contrast, KNU-141112-P5-challenged piglets (group 1) exhibited clinical signs including lethargy and diarrheic feces by 1 DPI (mean CSS of 0.33), and experienced severe watery diarrhea with vomiting thereafter (mean CSS of > 3.0) (Fig. 4A). PEDV-associated mortality occurred in all inoculated animals in group 1 at 4 or 5 DPI. Strikingly, the cell-adapted DEL virus-inoculated piglets in groups 2 and 3 underwent neither PEDV-specific clinical symptoms nor death throughout the experiment, even though some pigs inoculated with KNU-141112-S DEL2/ORF3 had mild and fluidic feces at 2 and 3 DPI. All inoculated piglets in group 1 were positive for PEDV, as determined by RT-PCR, by 1 DPI with a mean Ct value of 29.88 (equivalent to $10^{2.25}$ $TCID_{50}$/ml), and they shed increasingly amounts of PEDV in feces with Ct ranges of 8.49–12.02 ($10^{5.17}$–$10^{5.74}$ $TCID_{50}$/ml) until they died (Fig. 4B). PEDV fecal shedding was recorded in all piglets in groups 2 and 3 by 2 DPI with the mean Ct values of 21.96 ($10^{3.54}$ $TCID_{50}$/ml) and 30.11 ($10^{2.21}$ $TCID_{50}$/ml), respectively, and similarly reached peak levels at 4 DPI, with a gradual decline thereafter. Overall, the quantities of virus in feces in animals of groups 2 and 3 significantly declined relative to that in the group 1 animals, with wide Ct ranges of 28.67–17.58 ($10^{2.45}$–$10^{4.26}$ $TCID_{50}$/ml) and 31.77–21.33 ($10^{1.94}$–$10^{3.64}$ $TCID_{50}$/ml), respectively, until the termination of the study, indicating limited shedding (more than a 2-log reduction) of the S DEL2/ORF3 and S DEL5/ORF3 strains. Negative control pigs remained active with normal feces and no detectable PEDV shedding in feces throughout the experimental period.

All piglets in the parental KNU-141112-P5-infected group were necropsied upon death at 4 or 5 DPI. Entire animals in the remaining groups were euthanized at the end of the study for postmortem

assessments (Fig. 4C). Neither macroscopic nor microscopic intestinal lesions were observed in the negative control piglets (panel vi). All pigs inoculated with a virulent KNU-141112-P5 strain macroscopically displayed archetypal PED-like gross lesions. Their small intestines were dilated with accumulated yellow fluid and had thin transparent walls as a result of villous atrophy (panel v). Their stomachs were distended and filled with curdled undigested milk, whereas the other intestinal organs appeared grossly normal. In contrast, all animals infected with cell-adapted KNU-141112-S DEL2-ORF3 or KNU-141112-S DEL5-ORF3 in groups 2 and 3, respectively, showed no remarkable visible pathological lesions in their gastrointestinal tracts, similar to those in the negative control group (panels i–iv). Microscopic assessment showed that the small intestines from all dead piglets in group 1 were characterized by acute viral enteritis, with shortening and fusion of small intestinal villi and vacuolation of superficial epithelial cells (Fig. 5E). Furthermore, IHC staining revealed that PEDV antigen was predominant in the cytoplasm of epithelial cells in atrophied villi in all segments of the small intestines (Fig. 5K). However, the cell-adapted virus-inoculated pigs in groups 2 and 3 exhibited normal intestinal histopathologies, comparable to those of the negative control group (Figs. 5A–D). No virus antigen was present in the small intestines in any animals in groups 2 and 3 (Figs. 5G–J). Altogether, our data indicates that cell-adapted KNU-141112-S DEL2-ORF3 and KNU-141112-S DEL5-ORF3 possessed noticeably weakened virulence with clearly attenuated phenotypes in experimentally inoculated piglets.

Next, we aimed to evaluate the immunogenicity of the attenuated strains in the natural host. Antisera were collected from the pigs before immunization (pre-immune) and at 2 weeks after the final boost with each virus, and they were tested for neutralizing activity against the isolate KNU-141112. The serum samples obtained from pigs immunized with the cell-adapted KNU-141112-S DEL2-ORF3 or KNU-141112-S DEL5-ORF3 strain were highly effective in inhibiting KNU-141112-P5, with geometric mean neutralizing antibody titers of 1:64 or 1:128, respectively, which are comparable to the response of the antisera against the parental virus. Conversely, none of the pre-immune or non-immunized sera showed neutralizing activity against PEDV. Taken together, our data indicates that the cell-attenuated KNU-141112-S DEL2-ORF3 and KNU-141112-S DEL5-ORF3 strains can elicit robust antibody responses in immunized animals, thereby inducing protective immunity against PEDV infection.

4. Discussion

Since the sudden emergence of PEDV in the US, this viral agent has become globally renowned and is now considered an emerging or re-emerging pathogen with economic effects on the world pork business. In South Korea, despite substantial efforts, including a nationwide vaccination campaign for PEDV control, this devastating virus has menaced the domestic swine industry over the last two decades and become endemic, thereby causing continuous financial disbenefits. To prevent emerging and re-emerging PEDV-associated epizootics and enzootics, it is critical not only to continue monitoring and characterizing the virus circulating in pig-producing regions but also to make unremitting exertion of the development of more effective vaccines. Our circumstances have increased the need for safe and efficient next-generation PEDV vaccines based on field epizootic strains. We recently isolated and propagated a Korean high entero-pathogenic PEDV strain in Vero cells that is genotypically identical to the G2b global field strains (Lee et al., 2015). In the present study, we obtained PEDV MLV vaccine candidates by 100 passages of the virulent KNU-141112 strain in Vero cells and ascertained the genetic and pathogenic characteristics of these strains. An initial sequencing analysis using the traditional Sanger method verified four cell-adapted variants that each contained small DEL patterns in the N-terminal part of S (S DEL2 and S DEL5) or a combination of S DEL and a large DEL in the intergenic junction between S and ORF3 (S DEL2/ORF3 and S DEL5/ORF3). The virological assays revealed that the cell-adapted DEL viruses grew more efficiently and formed larger plaques than the parental virus in cultured cells. The parental KNU-141112-P5 virus generated homogeneous pinpoint-sized plaques, whereas DEL strains each produced heterogeneous plaques (a mix of at least two sizes) (Fig. 1D). S DEL2 infection resulted in the formation of small, relatively homogeneous plaques in Vero cells, whereas the S DEL5 strain formed a mixture of tiny-, medium-, and large-sized plaques. Intriguingly, the S DEL2/ORF3 and S DEL5/ORF3 strains exhibited almost identical large plaques, along with a few tiny plaques. Altogether, these findings indicate that the cell-adapted DEL strains had a superior viral fitness in the cultured cells and that DEL patterns positively influenced *in vitro* viral growth.

Subsequently, we sequenced the entire genomes of the DEL strains to decode the precise DEL patterns and genetic mutations that emerged during serial cell passage. Upon cell adaptation, a total of 12 or 14 non-synonymous mutations arose in ORFs 1 through 4. Interestingly, 6 aa substitutions were accumulated in the nonstructural viral proteases nsp3 and nsp5 and structural proteins S and E of all DEL strains, suggesting that some of these changes are associated with virus adaption in the cell cultured system. The S protein can be divided into four structural domains: a signal peptide, a large external domain that is further separated to two subdomains (S1 and S2), a transmembrane domain, and a short carboxyl terminal cytosolic/virus-internal endodomain (Lai et al., 2007). The S protein induces fusion of the viral envelope with host cell membranes, and this membrane fusion activity is most like conferred by the internal hydrophobic sequences in the S2 portion (Lai et al., 2007; Lee, 2015). The cell-adapted strains formed more extensive syncytia, resulting in an increase in vacuolated areas that were proportional to plaque sizes. Since all DEL strains contained G888R and E1287Q mutations in the S2 fusion domain, these genetic drifts may contribute to cytopathology. In the S protein of PEDV, two neutralizing epitopes have been identified at aa positions 748–755 and 764–771 (Sun et al., 2008). The aa residues that comprise these epitopes remained unchanged throughout cell passages. The PEDV S protein is heavily glycosylated, and the parental KNU-141112-P5 strain contains 21 potential N-glycosylation sites defined by N-X-S/T, where X is any aa except proline. All of the cell-adapted DEL strains were found to contain either an N381K or T383N mutation in the N-S-T glycosylation sequon at positions 381 to 383 of the parental virus S protein. Additionally, the S DEL2/ORF3 strain lost one more potential sequon (NIT at positions 514 to 516 of S) by containing a strain-specific T516I change. Consequently, 20 or 19 N-glycosylation sites were predicted in the DEL strains, with one or two missing motif(s), respectively. This finding is consistent with those of previous studies, but inconsistent in that a new motif, in close proximity site or at a distinct location, was created to compensate the loss in other cell-attenuated strains, resulting in an identical number of the N-glycosylation sites (Park et al., 2007; Sato et al., 2011). One or two altered glycan motifs can influence the pathogenicity of the cell-adapted DEL strains, whereas the conservation of the other N-glycosylation sites implies the significance of N-linked glycosylation in the S protein for the protein conformation and function.

In addition to point mutations, we found the genesis of 4 different minor and/or major DEL signatures. The first S N-DEL2 or S N-DEL5 and the fourth ORF3 C-DEL1 were classified as minor DEL patterns because of the number of nt deletion at respective positions in S or ORF3. Compared with classical G1a strains, S genes of G2 epidemic field strains, including KNU-141112, are 9-nt (3-aa) longer, resulting from distinct genetic signatures, S insertions-deletions (S INDELs) consisting of two notable 4-aa and 1-aa insertions at positions 55/56 and 135/136, respectively, and a 2-aa deletion at positions 160 and 161 of S (Lee et al., 2010; Lee, 2015). The S N-DEL2 and S N-DEL5 patterns emerged at the first insertion footprint in S genes of G2 field strains, and, accordingly, the S N-DEL signatures of cell-adapted strains were analogous to those of the classical G1a strains, except for their lengths. The second pattern was a major DEL signature, with a large 46-nt deletion at genomic positions 24,771 through 24,816, spanning the junction between S and ORF3. Interestingly, this major DEL signature is almost the same as that present in the Korean cell-adapted vaccine

strain SM98-1 (GenBank accession no. GU937797), which possesses an extended 52-nt deletion at similar positions (Fig. 2B and C). Thus, SM98-1 is predicted to encode an alternate S protein with a 7-aa excised cytoplasmic domain that is two aa shorter than those of S DEL2/ORF3 and S DEL5/ORF3 and either no ORF3 or an N-DEL70-truncated ORF3 identical to that identified in this study. Additionally, another Korean vaccine strain, DR-13, also has a large 17-aa deletion at positions 82–98 in ORF3; this deletion resulted spontaneously from continuous nt deletions at the corresponding positions (Park et al., 2008). Lastly, the remaining DEL signature contained a massive 88-aa deletion in the C-terminus of ORF3 (ORF3 C-DEL88). Similarly, Wang et al. (2012) reported an attenuated PEDV that encodes a C-terminal-truncated ORF3 protein of 91 aa compared to the 224 aa in the wild-type virus. However, our finding differed in that the ORF3 gene of the attenuated virus in the previous study had a 49-nucleotide deletion, leading to a reading frame shift, and a TAG terminator at nt 274 of ORF3 farther upstream than the ORF3 C-DEL88 in the present study. More strikingly, with the exception of KNU-141112-S DEL2, the cell-adapted DEL strains contained the discontinuous multiple DEL signatures. As aforementioned, several cell-attenuated vaccine strains retain large deletions in ORF3 and encode truncated ORF3 variants, suggesting that this genotypic feature is associated with the loss of PEDV virulence.

Our experimental data indicate that both KNU-141112-S DEL2/ORF3 and KNU-141112-S DEL2/ORF3 are attenuated virologically and clinically *in vivo*. The findings from previous and present studies suggest that major genetic changes in ORF3 resulting from cell culture adaptation could be answerable for decreases in the pathogenicity of virulent PEDV strains, albeit contributions from other mutations or deletions, especially in the S gene, cannot be excluded. Although the exact function of PEDV ORF3 remains unknown, it has been proposed to consist of four transmembrane (TM) domains that form a tetrameric assembly (Wang et al., 2012). PEDV ORF3 has also been shown to encode an ion channel protein, and TM4 at aa positions 151–172 in ORF3 may be important for potassium channel activity (Wang et al., 2012). More interestingly, an attenuated PEDV that encodes a truncated ORF3 without the TM3 and TM4 domains was found to lack ion channel activity (Wang et al., 2012). However, one of the attenuated DEL strains, KNU-141112-S DEL5/ORF3, possesses a truncated ORF3 gene of 153 aa that is predicted to comprise domains TM2 to TM4 and, accordingly, to retain ion channel activity. Therefore, ion channel activity of the ORF3 product may be irrelevant to PEDV virulence. Specific knockdown of ORF3 by small interfering RNA (siRNA) in PEDV-infected cells reduced the number of virus particles in cells, indicating that ORF3 modulates virus production (Wang et al., 2012). Inconsistent with this previous work, we found that cell-adapted DEL strains with large deletions in ORF3 grew efficiently in cell culture. Moreover, a recent study also revealed that the PEDV ORF3 product is unnecessary for the replication of virus in cultured cells (Li et al., 2013). Taken together, data indicate that the accessory ORF3 gene is dispensable for PEDV replication *in vitro*. Despite an ignored function in virus propagation *in vitro*, conservation of the complete ORF3 in PEDV field isolates suggests that the ORF3 protein has a critical role in natural infection in the animal host.

In conclusion, we generated four distinct DEL strains through *in vitro* serial passage, and demonstrated the loss of virulence of cell-adapted viruses with heavy deletions in ORF3 *in vivo* and the retention of immunogenicity of these cell-attenuated strains in pigs. A growing body of evidence proposes that polygenic traits might be involved to correlate with phenotype properties of PEDV, but ORF3 may be an important viral component to determine the pathogenic features. Here, the data obtained from the current study showed that the cell-adapted S DEL2/ORF3 and S DEL5/ORF3 viruses were completely attenuated *in vivo*, indicating that the ORF3 defect resulting from extensive deletions may contribute to altered PEDV pathogenicity in the natural host. Further, the present work supports the notion that genetic changes associated with virulence hallmarks in PEDV are concentration in ORF3. However, it is still plausible that other genetic mutations identified in the attenuated DEL viruses are involved in the pathogenicity of PEDV, implying the multigenic character of PEDV virulence. Future work should aim to address the questions of whether genetic drifts in other genes, especially in nsps and S, influences PEDV virulence and what the specific role of the ORF3 protein is in viral replication and pathogenesis. Altogether, our findings provide insights into pioneering the development of a next generation live vaccine based on either the attenuated G2b S DEL2/ORF3 or S DEL5/ORF3 strain. To accomplish this task, our next step will be sow vaccination and challenge experiments to evaluate the protective efficacy of the vaccine candidate against virulent PEDV and to assess its safety concern in neonatal piglets.

Acknowledgment

This research was supported by Bio-industry Technology Development Program through the Korea Institute of Planning and Evaluation for Technology in Food, Agriculture, Forestry and Fisheries (iPET) funded by the Ministry of Agriculture, Food and Rural Affairs (315021-04).

References

Baek, P.S., Choi, H.W., Lee, S., Yoon, I.J., Lee, Y.J., Lee, D.S., Lee, S., Lee, C., 2016. Efficacy of an inactivated genotype 2b porcine epidemic diarrhea virus vaccine in neonatal piglets. Vet. Immunol. Immunopathol. 174, 45–49.

Boniotti, M.B., Papetti, A., Lavazza, A., Alborali, G., Sozzi, E., Chiapponi, C., Faccini, S., Bonilauri, P., Cordioli, P., Marthaler, D., 2016. Porcine epidemic diarrhea virus and discovery of a recombinant swine enteric coronavirus, Italy. Emerg. Infect. Dis. 22, 83–87.

Dastjerdi, A., Carr, J., Ellis, R.J., Steinbach, F., Williamson, S., 2015. Porcine epidemic diarrhea virus among farmed pigs, Ukraine. Emerg. Infect. Dis. 21, 2235–2237.

Grasland, B., Bigault, L., Bernard, C., Quenault, H., Toulouse, O., Fablet, C., Rose, N., Touzain, F., Blanchard, Y., 2015. Complete genome sequence of a porcine epidemic diarrhea S gene indel strain isolated in France in December 2014. Genome Announc. 3, e00535–15.

Hanke, D., Jenckel, M., Petrov, A., Ritzmann, M., Stadler, J., Akimkin, V., Blome, S., Pohlmann, A., Schirrmeier, H., Beer, M., Höper, D., 2015. Comparison of porcine epidemic diarrhea viruses from Germany and the United States, 2014. Emerg. Infect. Dis. 21, 493–496.

Kim, S.H., Kim, I.J., Pyo, H.M., Tark, D.S., Song, J.Y., Hyun, B.H., 2007. Multiplex real-time RT-PCR for the simultaneous detection and quantification of transmissible gastroenteritis virus and porcine epidemic diarrhea virus. J. Virol. Methods 146, 172–177.

Kim, S.H., Lee, J.M., Jung, J., Kim, I.J., Hyun, B.H., Kim, H.I., Park, C.K., Oem, J.K., Kim, Y.H., Lee, M.H., Lee, K.K., 2015. Genetic characterization of porcine epidemic diarrhea virus in Korea from 1998 to 2013. Arch. Virol. 160, 1055–1064.

Kocherhans, R., Bridgen, A., Ackermann, M., Tobler, K., 2001. Completion of the porcine epidemic diarrhoea coronavirus (PEDV) genome sequence. Virus Genes 23, 137–144.

Kweon, C.H., Kwon, B.J., Jung, T.S., Kee, Y.J., Hur, D.H., Hwang, E.K., Rhee, J.C., An, S.H., 1993. Isolation of porcine epidemic diarrhea virus (PEDV) in Korea. Korean J. Vet. Res. 33, 249–254.

Kweon, C.H., Kwon, B.J., Lee, J.G., Kwon, G.O., Kang, Y.B., 1999. Derivation of attenuated porcine epidemic diarrhea virus (PEDV) as vaccine candidate. Vaccine 17, 2546–2553.

Lai, M.M., Perlman, S., Anderson, L.J., 2007. Coronaviridae. In: Knipe, D.M., Howley, P.M., Griffin, D.E., Martin, M.A., Lamb, R.A., Roizman, B., Straus, S.E. (Eds.), Fields Virology, 5th ed. Lippincott Williams & Wilkins, Philadelphia, USA, pp. 1306–1336.

Lee, Y.N., Lee, C., 2013. Complete genome sequence of a novel porcine parainfluenza virus 5 isolate in Korea. Arch. Virol. 158, 1765–1772.

Lee, S., Lee, C., 2014. Outbreak-related porcine epidemic diarrhea virus strains similar to US strains, South Korea, 2013. Emerg. Infect. Dis. 20, 1223–1226.

Lee, D.K., Park, C.K., Kim, S.H., Lee, C., 2010. Heterogeneity in spike protein genes of porcine epidemic diarrhea viruses isolated in Korea. Virus Res. 149, 175–182.

Lee, S., Ko, D.H., Kwak, W.K., Lim, C.H., Moon, S.U., Lee, D.S., Lee, C., 2014a. Reemergence of porcine epidemic diarrhea virus on Jeju Island. Korean J. Vet. Res. 54, 185–188.

Lee, S., Park, G.S., Shin, J.H., Lee, C., 2014b. Full-genome sequence analysis of a variant strain of porcine epidemic diarrhea virus in South Korea. Genome Announc. 2, e01116–14.

Lee, S., Kim, Y., Lee, C., 2015. Isolation and characterization of a Korean porcine epidemic diarrhea virus strain KNU-141112. Virus Res. 208, 215–224.

Lee, C., 2015. Porcine epidemic diarrhea virus: An emerging and re-emerging epizootic swine virus. Virol. J. 12, 193.

Li, C., Li, Z., Zou, Y., Wicht, O., van Kuppeveld, F.J., Rottier, P.J., Bosch, B.J., 2013. Manipulation of the porcine epidemic diarrhea virus genome using targeted RNA recombination. PLoS One 8, e69997.

Lin, C.N., Chung, W.B., Chang, S.W., Wen, C.C., Liu, H., Chien, C.H., Chiou, M.T., 2014. US-like strain of porcine epidemic diarrhea virus outbreaks in Taiwan, 2013–2014. J.

Vet. Med. Sci. 76, 1297–1299.
Mesquita, J.R., Hakze-van der Honing, R., Almeida, A., Lourenço, M., van der Poel, W.H., Nascimento, M.S., 2015. Outbreak of porcine epidemic diarrhea virus in Portugal, 2015. Transbound. Emerg. Dis. 62, 586–588.
Mole, B., 2013. Deadly pig virus slips through US borders. Nature 499, 388.
Oh, J., Lee, K.W., Choi, H.W., Lee, C., 2014. Immunogenicity and protective efficacy of recombinant S1 domain of the porcine epidemic diarrhea virus spike protein. Arch. Virol. 159, 2977–2987.
Park, S.J., Moon, H.J., Yang, J.S., Lee, C.S., Song, D.S., Kang, B.K., Park, B.K., 2007. Sequence analysis of the partial spike glycoprotein gene of porcine epidemic diarrhea viruses isolated in Korea. Virus Genes 35, 321–332.
Park, S.J., Moon, H.J., Luo, Y., Kim, H.K., Kim, E.M., Yang, J.S., Song, D.S., Kang, B.K., Lee, C.S., Park, B.K., 2008. Cloning and further sequence analysis of the ORF3 gene of wild- and attenuated-type porcine epidemic diarrhea viruses. Virus Genes 36, 95–104.
Pensaert, M.B., Debouck, P., 1978. A new coronavirus-like particle associated with diarrhea in swine. Arch. Virol. 58, 243–247.
Rothberg, J.M., Hinz, W., Rearick, T.M., Schultz, J., Mileski, W., Davey, M., Leamon, J.H., Johnson, K., Milgrew, M.J., Edwards, M., Hoon, J., Simons, J.F., Marran, D., Myers, J.W., Davidson, J.F., Branting, A., Nobile, J.R., Puc, B.P., Light, D., Clark, T.A., Huber, M., Branciforte, J.T., Stoner, I.B., Cawley, S.E., Lyons, M., Fu, Y., Homer, N., Sedova, M., Miao, X., Reed, B., Sabina, J., Feierstein, E., Schorn, M., Alanjary, M., Dimalanta, E., Dressman, D., Kasinskas, R., Sokolsky, T., Fidanza, J.A., Namsaraev, E., McKernan, K.J., Williams, A., Roth, G.T., Bustillo, J., 2011. An integrated semiconductor device enabling non-optical genome sequencing. Nature 475, 348–352.
Sagong, M., Lee, C., 2011. Porcine reproductive and respiratory syndrome virus nucleocapsid protein modulates interferon-b production by inhibiting IRF3 activation in immortalized porcine alveolar macrophages. Arch. Virol. 156, 2187–2195.
Saif, L.J., Pensaert, M.B., Sestak, K., Yeo, S.G., Jung, K., 2012. Coronaviruses. In: Zimmerman, J.J., Karriker, L.A., Ramirez, A., Schwartz, K.J., Stevenson, G.W. (Eds.), Diseases of Swine, 10th ed. Wiley-Blackwell, Ames, IA, USA, pp. 501–524.
Saitou, N., Nei, M., 1987. The neighbor-joining method: a new method for reconstructing phylogenetic trees. Mol. Biol. Evol. 4, 406–425.
Sato, T., Takeyama, N., Katsumata, A., Tuchiya, K., Kodama, T., Kusanagi, K., 2011. Mutations in the spike gene of porcine epidemic diarrhea virus associated with growth adaptation in vitro and attenuation of virulence in vivo. Virus Genes 43, 72–78.
Song, D.S., Oh, J.S., Kang, B.K., Yang, J.S., Moon, H.J., Yoo, H.S., Jang, Y.S., Park, B.K., 2007. Oral efficacy of Vero cell attenuated porcine epidemic diarrhea virus DR13 strain. Res. Vet. Sci. 82, 134–140.
Steinrigl, A., Fernández, S.R., Stoiber, F., Pikalo, J., Sattler, T., Schmoll, F., 2015. First detection, clinical presentation and phylogenetic characterization of porcine epidemic diarrhea virus in Austria. BMC Vet. Res. 11, 310.
Stevenson, G.W., Hoang, H., Schwartz, K.J., Burrough, E.R., Sun, D., Madson, D., Cooper, V.L., Pillatzki, A., Gauger, P., Schmitt, B.J., Koster, L.G., Killian, M.L., Yoon, K.J., 2013. Emergence of Porcine epidemic diarrhea virus in the United States: clinical signs, lesions, and viral genomic sequences. J. Vet. Diagn. Invest. 25, 649–654.
Sun, D., Feng, L., Shi, H., Chen, J., Cui, X., Chen, H., Liu, S., Tong, Y., Wang, Y., Tong, G., 2008. Identification of two novel B cell epitopes on porcine epidemic diarrhea virus spike protein. Vet. Microbiol. 131, 73–81.
Suzuki, T., Murakami, S., Takahashi, O., Kodera, A., Masuda, T., Itoh, S., Miyazaki, A., Ohashi, S., Tsutsui, T., 2015. Molecular characterization of pig epidemic diarrhoea viruses isolated in Japan from 2013 to 2014. Infect. Genet. Evol. 36, 363–368.
Tamura, K., Dudley, J., Nei, M., Kumar, S., 2007. MEGA4: molecular evolutionary genetics analysis (MEGA) software version 4.0. Mol. Biol. Evol. 24, 1596–1599.
Theuns, S., Conceição-Neto, N., Christiaens, I., Zeller, M., Desmarets, L.M., Roukaerts, I.D., Acar, D.D., Heylen, E., Matthijnssens, J., Nauwynck, H.J., 2015. Complete genome sequence of a porcine epidemic diarrhea virus from a novel outbreak in Belgium, January 2015. Genome Announc. 3, e00506–15.
Thompson, J.D., Gibson, T.J., Plewniak, F., Jeanmougin, F., Higgins, D.G., 1997. The CLUSTAL X windows interface: flexible strategies for multiple sequence alignment aided by quality analysis tools. Nucleic Acids Res. 25, 4876–4882.
Vlasova, A.N., Marthaler, D., Wang, Q., Culhane, M.R., Rossow, K.D., Rovira, A., Collins, J., Saif, L.J., 2014. Distinct characteristics and complex evolution of PEDV strains, North America, May 2013–February 2014. Emerg. Infect. Dis. 20, 1620–1628.
Wang, K., Lu, W., Chen, J., Xie, S., Shi, H., Hsu, H., Yu, W., Xu, K., Bian, C., Fischer, W.B., Schwarz, W., Feng, L., Sun, B., 2012. PEDV ORF3 encodes an ion channel protein and regulates virus production. FEBS Lett. 586, 384–391.